Available online at www.sciencedirect.com
SCIENCE DIRECT
Polymer 47 (2006) 4105–4114
polymer
www.elsevier.com/locate/polymer

FTIR investigation of the influence of diisocyanate symmetry on the morphology development in model segmented polyurethanes

Iskender Yilgor [a,*], Emel Yilgor [a], I. Guclu Guler [a], Thomas C. Ward [b], Garth L. Wilkes [c]

[a] *Department of Chemistry, Koc University, Istanbul 34450, Turkey*
[b] *Department of Chemistry, Virginia Polytechnic Institute and State University, Blacksburg, VA 24061, USA*
[c] *Department of Chemical Engineering, Virginia Polytechnic Institute and State University, Blacksburg, VA 24061, USA*

Available online 7 March 2006

Abstract

Novel segmented polyurethanes with hard segments based on a single diisocyanate molecule with no chain extenders were prepared by the stoichiometric reactions of poly(tetramethylene oxide)glycol (M_n = 1000 g/mol) (PTMO-1000) and 1,4-phenylene diisocyanate (PPDI), *trans*-1,4-cyclohexyl diisocyanate (CHDI), bis(4-isocyanatocyclohexyl)methane (HMDI) and bis(4-isocyanatophenyl)methane (MDI). Time dependent microphase separation and morphology development in these polyurethanes were studied at room temperature using transmission FTIR spectroscopy. Solvent cast films on KBr discs were annealed at 100 °C for 15 s and microphase separation due to self organization of urethane hard segments was followed by FTIR spectroscopy, monitoring the change in the relative intensities of free and hydrogen-bonded carbonyl (C=O) peaks. Depending on the structure of the diisocyanate used, while the intensity of free C=O peaks around 1720–1730 cm^{-1} decreased, the intensity of H-bonded C=O peaks around 1670–1690 cm^{-1}, which were not present in the original samples, increased with time and reached saturation in periods ranging up to 5 days. Structure of the diisocyanate had a dramatic effect on the kinetics of the process and the amount of hard segment phase separation. While PPDI and CHDI based polyurethanes showed self-organization and formation of well ordered hard segments, interestingly no change in the carbonyl region or no phase separation was observed for MDI and HMDI based polyurethanes. Quantitative information regarding the relative amounts of non-hydrogen bonded, loosely hydrogen bonded and strongly hydrogen bonded and ordered urethane hard segments were obtained by the deconvolution of C=O region and analysis of the relative absorbances in C=O region.

Keywords: Polyurethane; Hydrogen bonding; Morphology

1. Introduction

Thermoplastic, segmented polyurethanes (TPUs) are very versatile materials, which can display properties ranging from very soft thermoplastic elastomers to strong, rigid thermoplastics depending on their chemical compositions, backbone structures and resultant microphase morphologies and find applications in many different fields, such as; textile fibers, adhesives, protective coatings, membranes and biomaterials [1–3]. Versatility of TPU technology stems from commercial availability of a very large number of starting materials for their synthesis. As a result, TPU synthesis, characterization and investigation of their structure–property relations have been a very active field of interest both for academic and industrial researchers for almost 50 years [4–6]. The potential impact of polyurethanes continues to be very strong and promising in many emerging fields, such as biomaterials and tissue engineering [7–9], optoelectronics [10], shape-memory materials [11,12], conducting polymers [13], molecular recognition [14], smart surfaces and others [15,16].

Interesting properties and performance of segmented, thermoplastic polyurethanes are strongly dependent on their phase separated microphase morphologies, which consists of domains of hard segments distributed in a continuous soft segment matrix [17–25]. It is generally believed that one of the most important factors or driving forces for the microphase separation in polyurethanes is the strong hydrogen bonding between the urethane hard segments [26–28]. However, as listed below, there are a very large number of chemical and structural factors, including the synthetic procedure followed and processing conditions, which play an important role in microphase separation or phase mixing. Important factors that influence TPU morphology include:

1. Chemical structure, number average molecular weight and molecular weight distribution of soft segments.

* Corresponding author. Tel.: +90 212 338 1418; fax: +90 212 338 1559.
E-mail address: iyilgor@ku.edu.tr (I. Yilgor).

0032-3861/$ - see front matter © 2006 Elsevier Ltd. All rights reserved.
doi:10.1016/j.polymer.2006.02.027

2. Chemical structure and symmetry of the diisocyanate.
3. Chemical structure of the chain extender, average chain length and length distribution of hard segments.
4. Hard/soft segment ratio in the copolymer.
5. Crystallizability of hard and soft segments.
6. Extent of competitive hydrogen bonding between hard–hard and hard–soft segments.
7. Inherent solubility between hard and soft segments.
8. Method/polymerization procedure used during the synthesis, which can be a one-step or two-step (prepolymer method).
9. The nature of the interfacial region between the soft segment matrix and hard segment domains.

With so many variables to consider, investigation of the morphological behavior of TPUs and interpretation of their structure–morphology–property behavior has been a very active but also a very challenging field of research since first reports by Schollenberger [4] and Cooper and Tobolsky [5]. During the past 40 years, there have been numerous studies and excellent publications on the preparation and structural, thermal, mechanical and morphological characterization of TPU systems by various research groups [4–6,17–28]. These efforts led to the development of various morphological models for segmented polyurethanes [17–25].

Unfortunately, due to the presence of so many factors and variables, quantitative determination of the extent of phase separation in TPUs has been a very difficult challenge. Recently, we reported the preparation and properties of novel segmented polyurethane and polyurea copolymers obtained by the stoichiometric reactions of hydroxy or amine terminated PTMO and various diisocyanates [29]. Microphase morphology and thermal and mechanical properties of these copolymers, which did not contain any chain extenders, showed very strong dependence on the symmetry of the diisocyanate. One of the most remarkable results of our work was the demonstration of the very important role played by the diisocyanate symmetry in the development of microphase separated morphology and resultant mechanical properties in polyurethanes. For this purpose, two homologous polyurethanes prepared by the stoichiometric reaction of PTMO-1000 and 1,3-phenylene diisocyanate (MPDI) and 1,4-phenylene diisocyanate (PPDI) have been investigated [29]. AFM studies showed well-defined microphase morphology in PPDI based polyurethane, whereas AFM images of the MPDI based homologous polyurethane was featureless. In addition, while PPDI based polyurethane displayed very good tensile properties at room temperature, its MPDI based homolog formed a very sticky film with no mechanical integrity. Recently, we also demonstrated that the polyurethane produced from 1,4-phenylene diisocyanate (PPDI) and PTMO-1000 displayed time-dependent morphology development at room temperature after annealing at 60 °C [30]. Interestingly, the equilibrium morphology for PPDI-PTMO-1000 polyurethane was reached after about 5–7 days of aging at room temperature. In addition to PTMO-1000 we also prepared and investigated the structure–morphology–property behavior of model polyurethanes based on the stoichiometric reactions of PTMO-2000 and diisocyanates. Some of these materials also display microphase morphology and elastomeric properties. Publication of these results will be forthcoming.

The major aims of this investigation were; (i) to monitor and understand the time-dependent morphology development in polyurethanes, (ii) to understand the influence of diisocyanate chain symmetry on the kinetics and thermodynamics of microphase separation, and (iii) to quantitatively determine the microphase separated and ordered hard segment content of these polyurethanes. For this purpose, we designed and synthesized polyurethanes with a minimum number of structural variables. They contained unimodal hard segments, which consisted of the diisocyanate only. In fact, the only variable was the molecular weight distribution of the PTMO. Model urethane compounds were also prepared by end-capping reactions of diisocyanates with *n*-butanol. These crystalline compounds were used as references in FTIR studies in order to determine the peak positions for completely phase separated and ordered urethane hard segments.

2. Experimental

2.1. Materials

Bis(4-isocyanatocyclohexyl)methane (HMDI) and bis(4-isocyanatophenyl)methane (MDI) were kindly provided by Bayer AG. 1,4-Phenylene diisocyanate (PPDI) was purchased from Aldrich. *trans*-1,4-Cyclohexyl diisocyanate (CHDI) was purchased from Du Pont. All diisocyanates, except PPDI were used as received. PPDI was sublimed at 70 °C. Purities of diisocyanates were better than 99.5%. Poly(tetramethylene oxide)glycol, with $\langle M_n \rangle$ 975 g/mol was kindly provided by DuPont. Reagent grade terephthaloyl chloride, *n*-butanol, *n*-butylamine, acetone, tetrahydrofuran (THF), toluene and dimethylformamide (DMF) were purchased from Aldrich and used as received. Dibutyltin dilaurate (T-12) was a product of Air Products.

2.2. Polymer synthesis

Polymerizations were conducted in three-neck, round bottom, Pyrex reaction flasks equipped with an overhead stirrer, reflux column and nitrogen inlet. All copolymers were prepared by the reaction of equimolar amounts of diisocyanate and PTMO-1000 in DMF or THF at 60 °C. No chain extenders were utilized. In reactions with aliphatic diisocyanates, 100 ppm of T-12 was used as catalyst. In a typical polymerization reaction (based on PPDI), 1.60 g (10.0 mmol) of PPDI and 9.75 g of PTMO-1000 (10.0 mmol) were introduced into a 250 mL Pyrex reaction vessel and dissolved in 10.0 g of DMF. Clear solution obtained was stirred and heated to 60 °C. As the molecular weight of the polymer formed and the solution viscosity increased with conversion, the reaction mixture was diluted with 15.0 g of DMF. Completion of the reactions was determined by monitoring the disappearance of the isocyanate absorption peak around

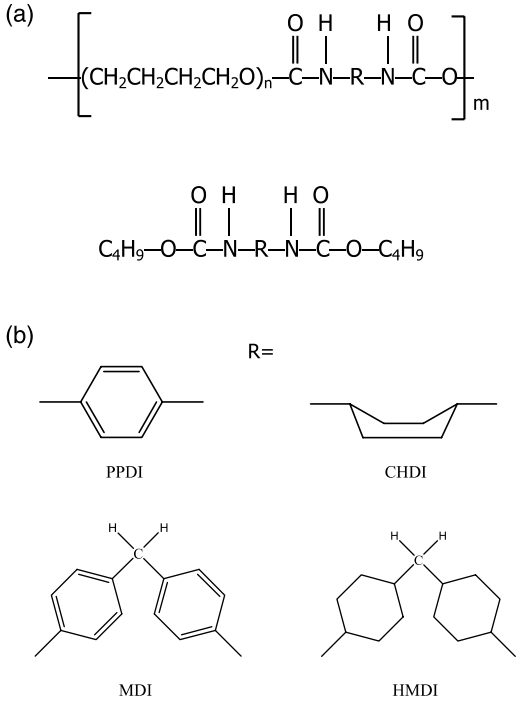

Fig. 1. (a) Chemical structures of the single diisocyanate based polyurethanes, (b) chemical structures of the model urethane compounds.

2270 cm^{-1} by FTIR. Chemical structures of the polyurethanes synthesized and investigated in this study are provided on Fig. 1(a). Chemical compositions, hard segment contents and average molecular weights of polyurethanes obtained are provided in Table 1. GPC results clearly demonstrate the formation of high molecular weight polymers.

2.3. Preparation of model compounds

Model urethane compounds were prepared by the reaction of PPDI, CHDI and HMDI with a 5-fold excess of *n*-butanol in DMF at 60 °C under the catalytic action of 100 ppm of T-12. Reactions were conducted in a two-neck round bottom Pyrex flask equipped with an overhead stirrer and nitrogen inlet. Model PPDI-urea compound was prepared in DMF, by the slow addition of *n*-butylamine into a PPDI solution at room temperature, under strong agitation. Model ester compound (dibutyl terephthalate) was prepared in toluene by the reaction of terephthaloyl chloride with a 5-fold excess of *n*-butanol, under strong nitrogen flow. Chemical structures of the model urethane compounds are provided in Fig. 1(b). Completion of the reactions for model compound synthesis was confirmed by FTIR spectroscopy. Products were coagulated in triple distilled water and washed with acetone several times before drying in a vacuum oven at 60 °C. Formation of the desired structures was confirmed by ^{1}H NMR spectroscopy and elemental analysis. Thermal characterization of model compounds was obtained by differential scanning calorimetry (DSC). Molecular weights, melting points and heat of fusion values of the model urethane compounds are provided in Table 2.

Table 1
Compositions and GPC molecular weights of polyether–urethanes obtained by the stoichiometric reactions between PTMO-1000 and various diisocyanates

Polymer Code	Diisocyanate	HS content[a] (wt%)	$\langle M_n \rangle$ (g/mol)	$\langle M_w \rangle$ (g/mol)	PDI (M_w/M_n)
HMDIPU	HMDI	21.2	46,000	72,000	1.57
PPDIPU	PPDI	14.1	47,000	70,000	1.49
MDIPU	MDI	20.4	36,000	52,000	1.44

[a] Hard segment (HS) content is the weight percent of diisocyanate in the polymer calculated from the stoichiometry of the reaction.

Table 2
Melting points and heat of fusion values of model urethane compounds

Model compound	Molecular weight[a] (g/mol)	Melting point (°C)	ΔH(fusion) (J/g)	ΔH(fusion) (kJ/mol)
BuO–HMDI–OBu	410.6	120	86.9	35.7
BuO–PPDI–OBu	308.4	158	114.5	35.3

[a] Theoretical value based on well-defined reaction, which is also confirmed by ^{1}H NMR.

2.4. Product characterization

Fourier transform infrared (FTIR) spectra were recorded on a Nicolet model Impact 400D FTIR spectrometer. FTIR scans were collected on thin films cast on KBr discs from THF solution, which were first dried and then heated to about 100–105 °C for 30 s with a heat gun. All spectra were collected using 20 scans with a resolution of 2 cm^{-1}. ^{1}H NMR spectra were collected in *d*-DMSO solution, on a Varian Unity 400 MHz spectrometer at ambient temperature. Gel permeation chromatography (GPC) measurements were conducted on a Waters system equipped with three inline PLgel 5 mm Mixed-C columns, an autosampler, a 410 RI detector, a Viscotek 270 dual detector, and an inline Wyatt Technologies miniDawn multiple angle laser light scattering (MALLS) detector at 40 °C in THF at 1 mL min^{-1}. Polystyrene standards were used for the calibration. Differential scanning calorimetry (DSC) analyses of the products were obtained on a TA DSC-100 instrument, under nitrogen atmosphere with a heating rate of 10 °C/min. Temperature and enthalpy calibration of DSC was obtained by using indium, lead and tin standards.

3. Results and discussion

Interesting solid-state properties of TPUs are explained by the microphase separation between hard and soft segments. In general, elastomeric TPUs contain 60–70% by weight of soft segments. Microphase morphologies of such elastomeric TPUs consist of a continuous soft segment matrix and hard segment domains. Interestingly, our recent work on the AFM investigation of model polyurethanes prepared by stoichiometric reactions between PTMO and diisocyanates, with ca. 15% by weight hard segment content, demonstrated the formation of microphase morphologies with interconnected hard segments that percolated through the soft matrix. In general, the lack of any competitive hydrogen bonding between hard and soft segments as in the case of siloxane–urea [31] or

hydrogenated butadiene–urea copolymers [32] favor the formation of well-separated microphase morphologies. Good microphase separation results in the formation of thermoplastic elastomers with excellent mechanical properties. On the other hand, it has been demonstrated that amorphous urethane hard segments show complete miscibility with amorphous polyethers at every composition [33,34]. Such systems show poor elastomeric properties. In general, highly polar urea hard segments are reported to promote phase separation and also provide more effective hydrogen bonding between the hard segments [35–37]. This also results in the formation of very high strength and high performance elastomers.

Although there is a general agreement on the two-phase morphologies of TPUs, there is limited information on the kinetics of phase separation and quantitative information on the composition (or purity) of the hard and soft segment microphases. In this report, we present our results on the FTIR investigation of time-dependent microphase separation in segmented polyurethanes prepared without chain extenders and we particularly address (i) influence of diisocyanate chain symmetry on the kinetics and thermodynamics of phase separation, and (ii) a quantitative measure of various microphases and their amounts in TPUs at equilibrium.

3.1. FTIR studies on model ester, urethane and urea compounds

Infrared spectroscopy is a simple but powerful technique for the investigation of hydrogen bonding in carbonyl compounds. This is clearly demonstrated in Fig. 2, where the carbonyl region of the FTIR spectra for homologous model ester (PPDIE), urethane (PPDIU) and urea (PPDIUr) compounds based on 1,4-phenylene core and butyl end groups are provided. All compounds show well-defined, strong and symmetrical carbonyl absorption bands, in a fairly broad wavenumber range of 1610–1760 cm^{-1}, depending on their hydrogen bonding capacities [25–28,37–39]. The peak maximum of the ester carbonyl, which cannot form hydrogen bonding, is at 1722 cm^{-1}. The urethane compounds, which can form medium to strong hydrogen bonding [38] has its carbonyl

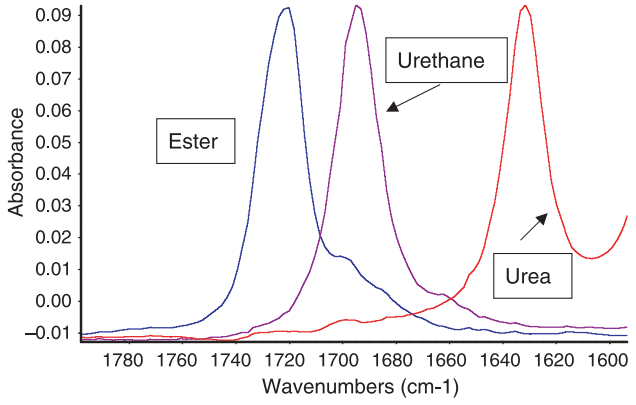

Fig. 2. Carbonyl region of the FTIR spectra for homologous model ester (PPDIE), urethane (PPDIU) and urea (PPDIUr) compounds based on 1,4-phenylene core and butyl end groups.

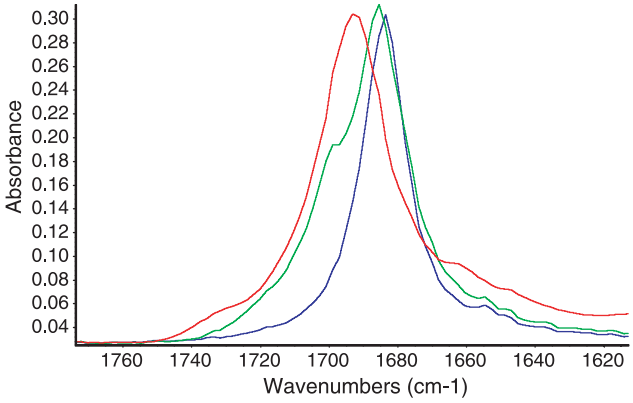

Fig. 3. Carbonyl regions of the FTIR spectra for model urethane compounds based on PPDIU (red), CHDIU (blue) and HMDIU (green).

peak maximum at 1695 cm^{-1}, whereas, the urea compound which can form very strong, bidentate hydrogen bonding [39], shows a peak maximum at 1635 cm^{-1}, much lower than that of the ester or urethane. Exact positions of the carbonyl peaks in urethanes based on different diisocyanates also show small differences. Carbonyl region of the FTIR spectra for model urethane compounds based on PPDI, CHDI, HMDI are reproduced in Fig. 3. The carbonyl peak for the compound based on aromatic and symmetrical PPDIU is at 1695 cm^{-1}. Interestingly, the carbonyl peak for a homologous urethane compound based on aliphatic and symmetrical CHDIU is at a slightly lower wavenumber of 1683 cm^{-1}. The urethane compound based on HMDI, an aliphatic but unsymmetrical diisocyanate shows a fairly sharp peak with maxima at 1685 cm^{-1}, which also has a distinct shoulder at 1695 cm^{-1}. This shoulder is most probably due to the presence of several isomers in HMDI, such as *trans*,*trans* (*E*,*E*), *trans*,*cis* (*E*,*Z*) and *cis*,*cis* (*Z*,*Z*). HMDI isomers influence the packing in the solid state and, in turn, the crystal structure of model urethane. This in turn prevents the formation of the well-ordered hydrogen bonded structure. In contrast we believe the sharp peak with maxima at 1685 cm^{-1} is in fact, representative of well-ordered hydrogen bonded structure, whereas the shoulder at 1695 cm^{-1} is due to imperfect hydrogen bonding.

When the FTIR spectra of model urethane compounds and model polyurethanes based on the same diisocyanate are compared, a very interesting behavior is observed. The carbonyl region of the FTIR spectra for the HMDIPU copolymer and model urethane BuO–HMDI–OBu are reproduced in Fig. 4. Although the chemical structures of the urethane groups are identical in both compounds, there is a remarkable difference in the C=O region of their FTIR spectra. Analysis of the differences in the C=O region of the FTIR spectra provides valuable information in understanding the extent of microphase separation in polyurethanes [25–28,37–39] and makes FTIR an important tool in the investigation of the microphase separation (and/or mixing) between hard and soft segments in polyurethanes. As discussed already and reproduced on Fig. 4, the model urethane shows a fairly sharp peak with a maximum at 1685 cm^{-1} and a shoulder at 1695 cm^{-1}. On the other hand, HMDIPU copolymer shows a

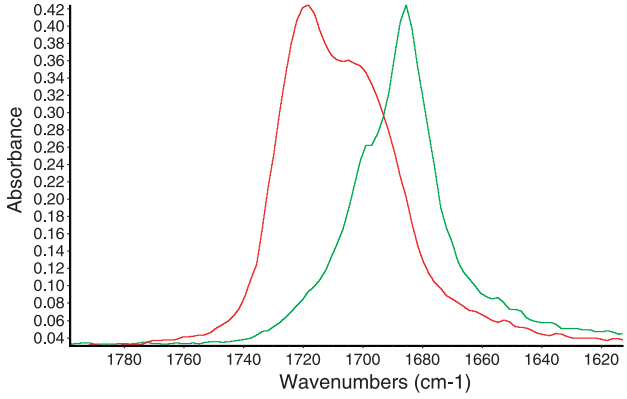

Fig. 4. Carbonyl regions of the FTIR spectra for HMDIPU copolymer (red) and model urethane BuO–HMDI–OBu (green).

very broad absorption band between 1650 and 1750 cm^{-1} range, with the peak maxima centered at 1720 cm^{-1} and a broad shoulder centered at 1705 cm^{-1}. The peak at 1720 cm^{-1}, which is very close to that of the ester carbonyl (1722 cm^{-1}) indicates the presence of substantial amount of non-hydrogen bonded urethane groups in HMDIPU. On the other hand, the broad shoulder at 1705 cm^{-1} indicates the presence of hydrogen bonded, disordered urethane groups [27,28] in the polymer. Interestingly, there is no peak at 1685 cm^{-1} in the model polyurethane indicating that there is no formation of well-ordered and strongly hydrogen bonded urethane groups in the polymer. These results clearly indicate extensive interaction between the ether oxygen in PTMO and the carbonyl group in the urethanes. This prevents the formation of a microphase-separated morphology in the solid state for HMDIPU and results in a polymer with no significant mechanical strength.

3.2. Influence of the diisocyanate structure on the time-dependent organization of the hard segments in polyurethanes based on PTMO-1000, containing no chain extenders

Recently, we reported the important role played by the diisocyanate chain symmetry in the structure–morphology–property behavior of segmented polyurethanes and polyureas [29]. In order to further understand the 'symmetry' effect on the self-organization of hard segments in polyurethanes, we investigated the time-dependent changes in the FTIR spectra of a series of homologous polyurethanes. For this purpose, we designed and synthesized polyurethanes with a minimum number of structural variables. They all had PTMO-1000 soft segments and contained unimodal hard segments, which consisted of the diisocyanate only. Diisocyanates used were CHDI, HMDI, PPDI and MDI. In fact, the only variable was the molecular weight distribution of the PTMO-1000. It should be noted that symmetrical CHDI and PPDI are the aliphatic and aromatic versions of the same basic ring structure. The HMDI and MDI based copolymers have similar structural relationships, however, due to the presence of methylene groups both structures are kinked and since rings rotate freely around the C–C bonds they disrupt the planar symmetry and ordered packing.

3.3. Time dependent organization of hard segments in PPDIPU

AFM and ATR-FTIR studies on the segmented PPDIPU (Table 2) clearly indicated a time-dependent morphology development in this copolymer [30]. Since AFM and ATR-FTIR are mainly surface sensitive techniques, we have utilized transmission FTIR in order to find out if a similar time-dependent organization and morphology development was also taking place in bulk. Time-dependent FTIR investigation was done using a thin film of PPDIPU cast on KBr disc from THF solution. In order to disrupt any structural organization (or microphase morphology) in the PPDIPU film, the sample was subjected to a temperature of 105 °C for 15 s. This temperature was chosen because it was about 50 °C above the melting point of oligomeric PTMO-1000 and 40 °C above the flow temperature of this polymer as obtained by DMA studies [30]. Immediately after this thermal treatment the sample was placed into the spectrometer and at $t=0$ min, the spectrum was recorded. FTIR spectrum of the sample was recorded at different time intervals up to 10 days. Between the scans the sample was kept in a dessicator at 23 °C. Two different regions of the FTIR spectra for PPDIPU samples at the $t=0$ (red spectrum) and $t=14400$ min (blue spectrum) aged at 23 °C, are

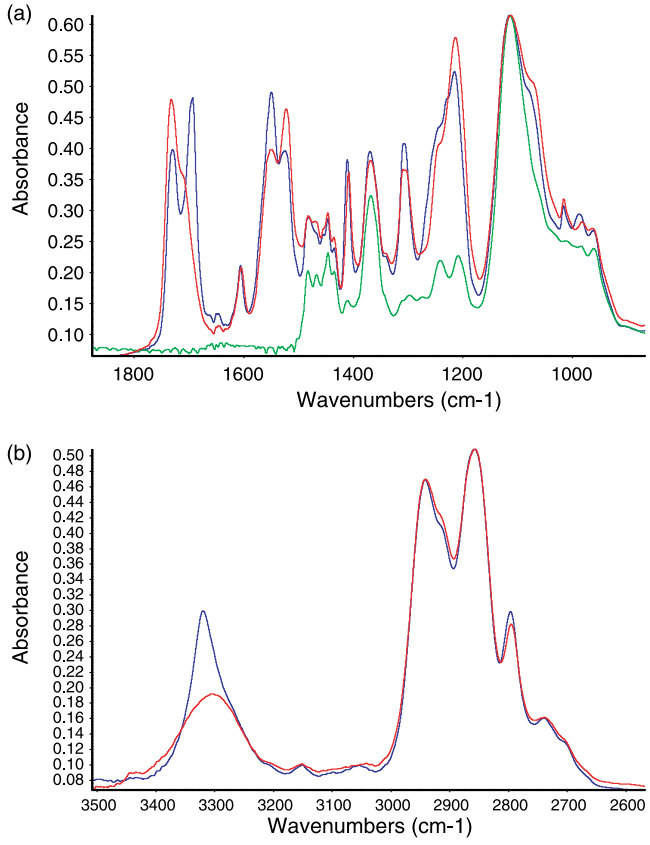

Fig. 5. (a) 900–1800 cm^{-1} and (b) 2600–3500 cm^{-1} regions of the FTIR spectra for PPDIPU at $t=0$ (red) and $t=14400$ min (blue) at 23 °C and PTMO-1000 (green).

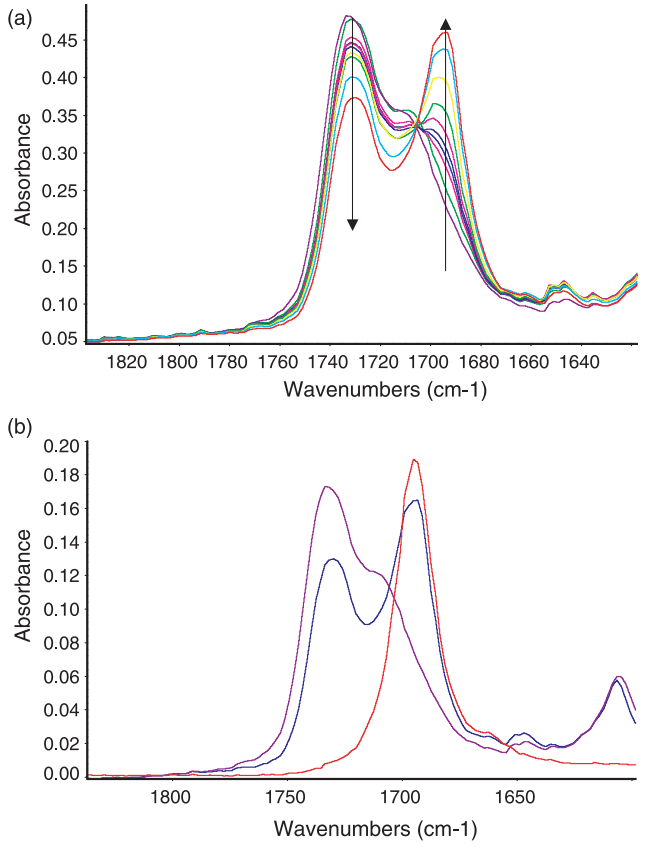

Fig. 6. Time dependent change in the carbonyl region of the FTIR spectra for PPDIPU from $t=0$ to 8200 min (a). Carbonyl region of the FTIR spectra for PPDIPU copolymer at $t=0$ (purple), $t=8200$ min (black) and the model urethane BuO–PPDI–OBu (red) (b).

reproduced in Fig. 5(a) (900–1800 cm^{-1}) and Fig. 5(b) (2600–3500 cm^{-1}). The FTIR spectrum of PTMO-1000 (green) is also provided in Fig. 6(a) as a reference for the ether peak at 1114 cm^{-1}.

Dramatic differences between the $t=0$ and 14400 min spectra in the amide I and amide II region (1500–1800 cm^{-1}) can clearly be seen in Fig. 5(a). As will be demonstrated later in the paper, this is a direct result of the time-dependent phase separation of urethane hard segments in PPDIPU upon aging at room temperature. As observed in Fig. 5(a), at $t=0$ min the sample shows a very strong absorption peak at 1733 cm^{-1} (free C=O) and a shoulder at 1708 cm^{-1} (hydrogen bonded, disordered C=O). Interestingly, there is no peak at 1695 cm^{-1} indicating the presence of strongly H-bonded and ordered C=O groups in the $t=0$ min sample. After the sample is aged at ambient temperature for 14400 min or 10 days, the 1733 cm^{-1} peak becomes much smaller whereas a very strong peak centered at 1695 cm^{-1} appears, indicating the formation of strongly hydrogen bonded urethane hard segments. A reversal in the strengths of 1550 and 1523 cm^{-1} (amide II) peaks is also observed upon microphase separation at room temperature. Interestingly, no noticeable change in peaks between 1175 and 1425 cm^{-1} are observed. On the other hand, there are noticeable differences in the strong ether (C–O–C) absorption bands (peak maximum at 1114 cm^{-1}) between PTMO-1000 and PPDIPU at $t=0$ and 14400 min. PTMO-1000 (green spectrum in Fig. 5(a)) has a sharp and fairly symmetrical ether peak at 1114 cm^{-1}. The $t=0$ min sample (red spectrum) has a broader peak with peak maximum at 1114 cm^{-1}, but it also displays a well defined shoulder at 1072 cm^{-1}. The $t=$ 14400 min sample (blue spectrum) shows a slightly narrower ether peak compared to the $t=0$ sample with the same peak maximum, and a shoulder at 1080 cm^{-1}. We believe the well defined shoulder at 1072 cm^{-1} in the $t=0$ sample is due to the presence of ether groups that are hydrogen bonded with urethanes in the phase mixed system. As the system microphase separates ($t=14400$ min sample) this shoulder moves to slightly higher wavenumbers and becomes weaker. However, since the microphase separation is not complete, it does not disappear completely.

Time dependent change in the carbonyl region of the FTIR spectra for PPDIPU from $t=0$ to 8200 min (5.7 days) are provided in Fig. 6(a). FTIR spectra for $t=8200$ and 14400 min were identical, indicating the completion of morphology development in bulk in about 6 days. As clearly seen in Fig. 6(a), as the sample is aged at room temperature, the 1733 and 1708 cm^{-1} peaks slowly become smaller and a well-defined shoulder at 1695 cm^{-1} starts forming after about 120 min. This indicates the formation of an ordered urethane hard segment phase. A steady increase in the 1695 cm^{-1} peak and continued decrease in the absorbance values of 1733 and 1708 cm^{-1} peaks are observed over time until $t=8200$ min. Under ambient conditions the FTIR study indicates the completion of the urethane hard segment self-assembly and microphase separation and achievement of the equilibrium morphology for PPDIPU, in about 8200 min or 6 days. For a better understanding of the nature of the phase separated hard segments, the carbonyl region of the FTIR spectra for the $t=0$, $t=8200$ min samples and that of the model hard segment compound (BuO–PPDI–OBu) are provided in Fig. 6(b). It is very interesting to observe almost a complete match between the 1695 cm^{-1} peaks of the copolymer and the model compound, clearly demonstrating the formation of well microphase separated and ordered urethane hard segments in the PPDIPU segmented copolymer at equilibrium.

It might be also added here that the kinetics of the FTIR time dependence noted for the PPDI copolymer sample are also in line with our earlier work on the AFM time dependent morphological (microphase separation) recovery studies [30] as well as newer time dependent SAXS kinetic studies (not yet published) on the same system. Since both the FTIR and SAXS techniques investigate the bulk sample while that of AFM is a surface technique, the compilation of the data from these three methods nicely confirms that what is gleaned by each are all are in agreement with each other.

In spite of the presence of a well-organized urethane hard segment phase, a substantial amount of non-hydrogen bonded or poorly organized hydrogen bonded carbonyl groups are still present at equilibrium, as indicated by the sizes of the 1733 and 1708 cm^{-1} peaks in Fig. 6(b). In order to obtain a quantitative measure of the percent amounts of different carbonyl groups present and to determine the extent of hard segment phase

separation, time-dependent FTIR spectra between 1675 and 1750 cm^{-1} were analyzed by deconvolution of the C=O peaks by using the Peakfit Version 4.12 software package from Systat Software, Inc. The percentage of each C=O absorption was obtained by comparing the specific peak area with the total peak area at each scan. For comparison, a similar analysis was also performed by determining the relative absorbance values of different C=O peaks. In this analysis, the absorbance values of C=O peaks were converted to percentages by using the following equation, which provided the percentages of non-hydrogen bonded, hydrogen bonded, disordered and strongly hydrogen bonded and ordered hard segments.

$$\%C=O(\text{at } 1965) = \frac{A(1695)}{A(1733)+A(1708)+A(1695)}$$

The results of the C=O peak analysis for PPDIPU by peak deconvolution and by absorbance analysis are provided in Table 3. As can be seen in Table 3, the results obtained by deconvolution and absorbance analyses show some differences at the beginning, however, after about 90 min of aging the results obtained by both methods become fairly similar and are within the experimental error. This is expected, since the shape and especially the breadth or area of the FTIR peaks have strong influence on the deconvolution results, however, they have no effect on the absorbance analysis. As can be seen in Figs. 6 and 8, as the morphology develops the peaks become well defined and sharper, as a result they show better agreement with the absorbance analysis. For the $t=0$ min sample deconvolution results indicate the presence of a substantial amount of free carbonyl (60%), a reasonable amount of hydrogen bonded, disordered carbonyl (28%) and very small amount of strongly hydrogen bonded carbonyl groups (12%). Upon storage (aging) at room temperature, the amount of free carbonyl decreases while the amount of strongly hydrogen-bonded and ordered carbonyl increases substantially. Results of the deconvolution analysis for the PPDIPU copolymer are plotted in Fig. 7(a) (complete data) and (b) (up to 600 min). As can be seen from these figures, a major part of the morphological development takes place within the first 600 min or 10 h, which is consistent with our AFM results [20]. From Table 3 and Fig. 7(a), it is interesting to note that the equilibrium morphology of PPDIPU contains less than 50% of well microphase separated urethane hard segments. More importantly, according to Table 3 and Fig. 7(a), more than 30% of the urethane hard segments seem to be well mixed or dispersed within the PTMO matrix (1733 cm^{-1} peak) at the equilibrium morphology.

Table 3
Quantitative analysis of the carbonyl region of the time-dependent FTIR spectra for PPDIPU by peak deconvolution and relative absorbances

Time (min)	Analysis by peak deconvolution			Analysis by relative absorbances		
	1733 cm^{-1}	1708 cm^{-1}	1695 cm^{-1}	1733 cm^{-1}	1708 cm^{-1}	1695 cm^{-1}
0	60.0	28.0	12.0	47.5	34.9	17.6
20	56.3	30.1	13.6	46.1	34.5	19.4
40	52.1	32.6	15.3	44.6	33.7	21.6
60	48.6	33.3	18.1	43.5	32.7	23.8
90	44.6	35.1	20.3	42.2	31.9	25.9
120	43.4	35.4	21.2	41.5	31.2	27.3
150	42.3	34.3	23.4	41.0	30.8	28.2
180	41.2	33.9	24.9	40.5	30.4	29.2
240	40.5	32.0	27.5	39.8	29.8	30.4
330	40.0	28.0	32.0	39.0	29.3	31.7
460	39.5	26.0	34.5	38.5	28.6	32.9
600	38.2	25.5	36.3	37.9	28.0	34.2
1350	37.0	24.3	38.8	35.7	25.5	38.8
3150	36.0	23.2	40.8	34.2	24.5	41.2
5170	34.3	21.6	44.1	33.6	23.9	42.5
8200	32.5	20.5	47.0	33.1	23.5	43.4
9400	32.4	20.5	47.1	33.1	23.5	43.5

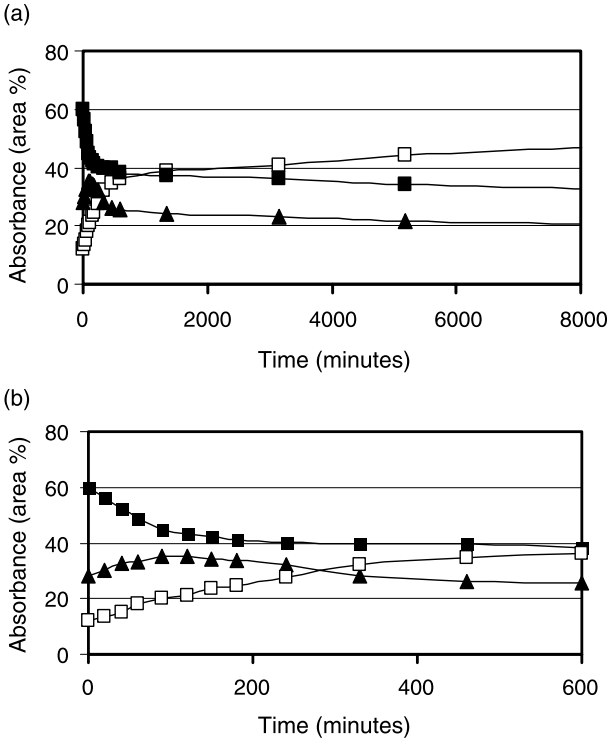

Fig. 7. Deconvolution results on the time-dependent changes in the relative amounts of carbonyl groups with different extent of hydrogen bonding in PPDIPU copolymer. Complete data (a) and up to 600 min (b).

3.4. Time-dependent organization of hard segments in CHDIPU, HMDIPU and MDIPU

We already reported the influence of diisocyanate chain symmetry on the thermal and mechanical properties of segmented polyurethanes obtained by the stoichiometric reactions between various diisocyanates and PTMO-1000 [29]. In order to understand the influence of diisocyanate structure (symmetry) on the morphology development, time dependent FTIR studies were conducted on CHDIPU, MDIPU and HMDIPU. Time-dependent FTIR spectra for the C=O and N–H regions of the CHDIPU copolymer are reproduced in Fig. 8(a) and (b), respectively. As can be seen in Fig. 8(a), a fairly broad, free C=O peak at 1732 cm^{-1} initially present in the system becomes smaller with time. On the other hand, a strongly hydrogen bonded C=O peak at 1685 cm^{-1}, which is initially present only as a shoulder becomes

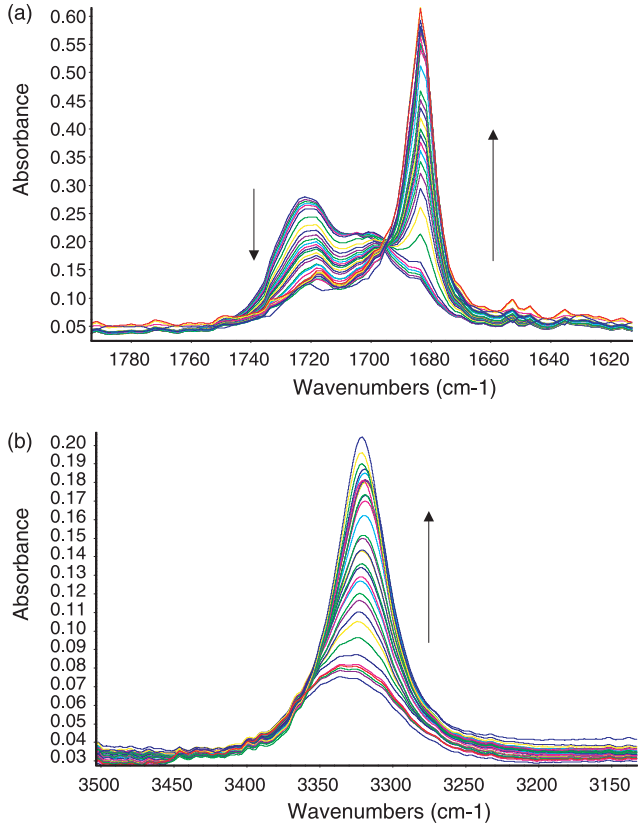

Fig. 8. Time dependent FTIR spectra for CHDIPU copolymer. C=O region (a) and N–H region (b).

stronger with time and reaches saturation in about 240 min, much faster than that of PPDIPU copolymer. Similarly, the initially broad and weak N–H peak (3250–3410 cm^{-1}) with maxima at 3336 cm^{-1}, becomes stronger and sharper (3250–3380 cm^{-1}) and the peak maxima moves to slightly lower wavenumbers (3321 cm^{-1}) as a result of hydrogen bonding within the urethane hard segments. Similar to the PPDIPU material the strongly hydrogen bonded C=O peak of CHDIPU matches the C=O peak of the model urethane CHDIU very well (Fig. 9), indicating very good microphase separation. Quantitative information on the time-dependent changes in the amount of different carbonyl absorptions in the CHDIPU material, obtained by the deconvolution of the peak areas are provided in Fig. 10(a) (complete data) and (b) (up to 40 min). As comparatively shown in Fig. 11, using the deconvolution results, it is very interesting to note that the rate of microphase separation due to the hydrogen bonding within urethane hard segments is much faster in the CHDIPU copolymer when compared with the homologous PPDIPU system. It is also important to note that at equilibrium (Figs. 7(a) and 10(a)), the extent of microphase separation of the (pure) urethane segments is higher in CHDIPU (65%), when compared with PPDIPU (47%).

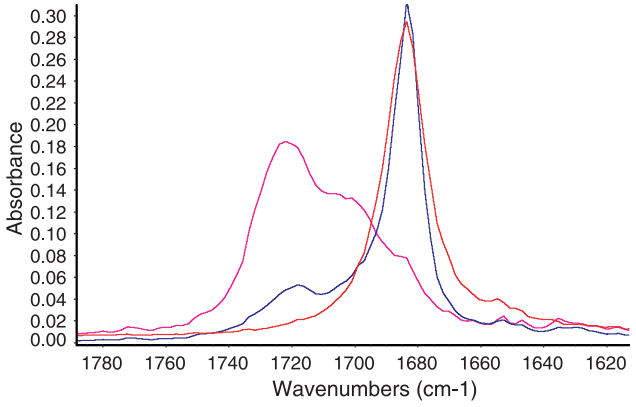

Fig. 9. Carbonyl region of the FTIR spectra for CHDIPU copolymer at $t=0$ (pink), $t=8200$ min (black) and the model urethane BuO–CHDI–OBu (red).

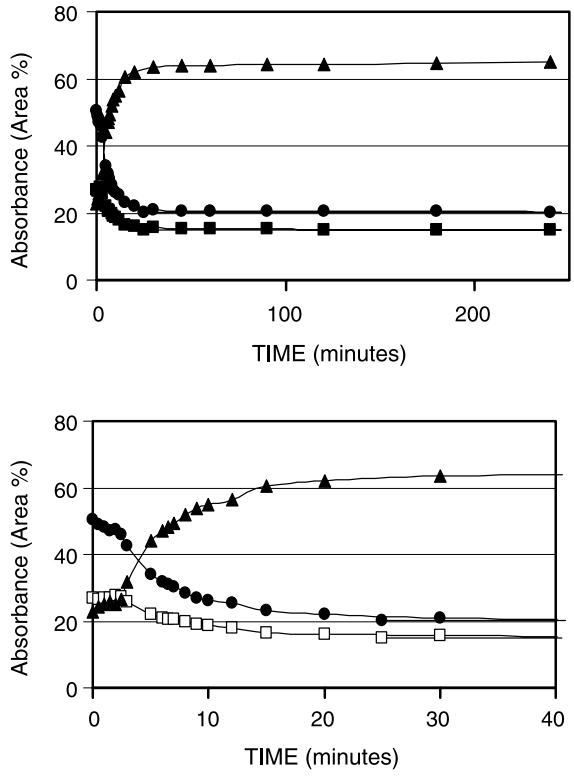

Fig. 10. Deconvolution results on the time-dependent changes in the relative amounts of carbonyl groups with different extent of hydrogen bonding in CHDIPU copolymer. Complete data (a) and up to 40 min (b).

Finally, the time-dependent FTIR behavior of two homologous polyurethanes prepared from unsymmetrical

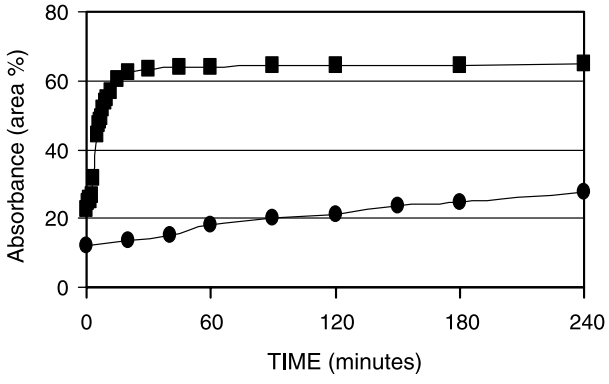

Fig. 11. Comparison of the time-dependent change in the carbonyl absorption peaks for well phase separated urethane groups in PPDIPU (●) and CHDIPU (■).

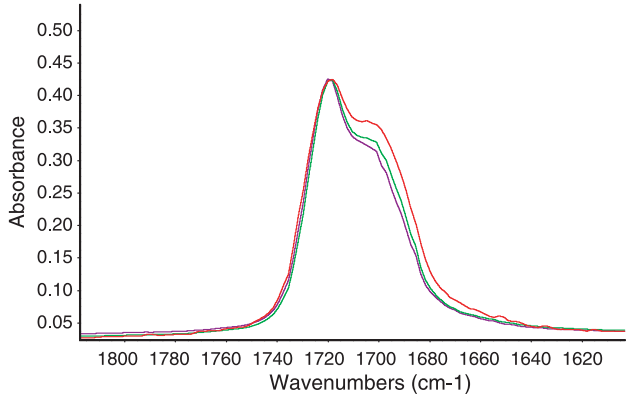

Fig. 12. Carbonyl region of the FTIR spectra for HMDIPU copolymer at $t=0$ (black), $t=60$ min (green) and $t=14400$ min (red).

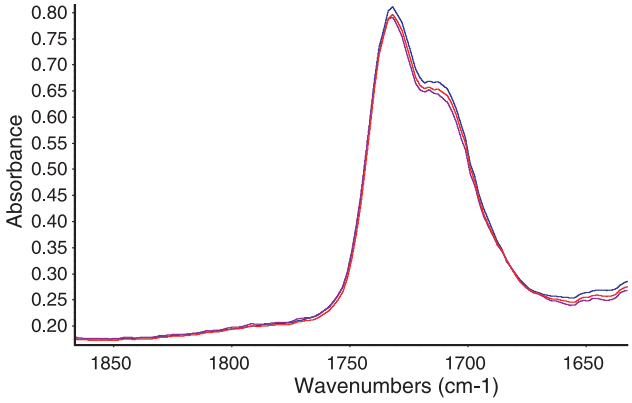

Fig. 13. Carbonyl regions of the FTIR spectra for MDIPU copolymer, $t=0$ min (black), $t=60$ min (red) and $t=14400$ min (blue).

diisocyanates were investigated. The carbonyl regions of the FTIR spectra for HMDIPU and MDIPU copolymers are provided in Figs. 12 and 13, respectively. It is very interesting to note that there was no change in the shape or position of the carbonyl peaks in either copolymer for up to 6 days, indicating no significant microphase separation.

4. Conclusions

We believe our FTIR investigations on the morphology development in PTMO-1000 based model polyurethanes obtained by the stoichiometric reactions of various diisocyanates (with no chain extenders) have several important ramifications, which can be summarized as follows:

(i) the kinetics of the hydrogen bonding between urethane hard segments leading to a microphase separated morphology strongly depend on the chemical structure and the symmetry of the diisocyanate.
(ii) in the equilibrium morphology the urethane hard segments are found in three different states or phases, these are; (a) well microphase separated (pure) and strongly hydrogen bonded hard segments, (b) loosely hydrogen bonded hard segments, and (c) non-hydrogen bonded (polyether mixed) hard segments.
(iii) the extent of the microphase separated urethane hard segments (in equilibrium morphology) is dependent on the symmetry of the diisocyanate, and
(iv) no significant microphase separation is observed in model, polyether urethanes (containing no chain extenders) based on kinked, asymmetric diisocyanates, such as MDI and HMDI.

In order to better understand the relative influences of hydrogen bonding and chain symmetry on the microphase separation and structure–morphology–property behavior of segmented copolymers, we also investigated the polyurea counterparts of these model polyurethanes. In polyureas, as expected, much more powerful, bidentate hydrogen bonding between urea hard segments played a more important role on the kinetics of microphase separation and thermal and mechanical properties of the copolymers. This word will be forthcoming in a separate publication.

References

[1] Woods G. The ICI polyurethanes book. New York, NY: Wiley; 1990.
[2] Lelah MD, Cooper SL. Polyurethanes in medicine. Boca Raton, FL: CRC Press; 1986.
[3] Aggarwal SL, editor. Block polymers. New York, NY: Plenum Press; 1970.
[4] Schollenberger CS, Scott H, Moore GR. Rubber World 1958;137:549–55.
[5] Cooper SL, Tobolsky AV. J Appl Polym Sci 1966;10:1837.
[6] Hicks Jr EM, Ultee AJ, Drougas C. Science 1965;147:373–9.
[7] Burke A, Hasirci N. Adv Exp Med Biol 2004;553:83–101.
[8] Guan JJ, Wagner WR. Biomacromolecules 2005;6(5):2833–42.
[9] Santerre JP, Woodhouse K, Laroche G, Labrow RS. Biomaterials 2005;26(35):7457–70.
[10] Demirbas U, Kurt A, Sennaroglu A, Yilgor E, Yilgor I. Polymer 2006;47.
[11] Lendlein A, Langer R. Science 2002;296(5573):1673–6.
[12] Ping P, Wang W, Chen X, Jing X. Biomacromolecules 2005;6(2):587–92.
[13] Chen WC, Chen HH, Wen TC, Digar M, Gopalan A. J Appl Polym Sci 2004;91(2):1154–67.
[14] Koevoets RA, Versteegen RM, Kooijman H, Spek AL, Sijbesma RP, Meijer EW. J Am Chem Soc 2005;127:2999–3003.
[15] Makal U, Uilk J, Kurt P, Cooke RS, Wynne KJ. Polymer 2005;46(8):2522–30 and Makal U, Fujiwara T, Cooke RS, Wynne KJ, Langmuir.
[16] Versteegen RM, Kleppinger R, Sijbesma RP, Meijer EW. Macromolecules 2006;39:772–83.
[17] Estes GM, Seymour RW, Cooper SL. Macromolecules 1971;4:452.
[18] Legge NR, Holden G, Schroeder HE, editors. Thermoplastic elastomers: a comprehensive review. New York, NY: Hanser Publishers; 1987.
[19] Hepburn C. Polyurethane elastomers. Essex: Elsevier Science Publishers Ltd; 1992.
[20] Abouzahr S, Wilkes GL. In: Folkes MJ, editor. Processing, structure and properties of block copolymers. London: Elsevier Applied Science Publishers; 1985. p. 165–207.
[21] Bonart RJ. Macromol Sci Phys 1968;B2(1):115–38.
[22] Wilkes CE, Yusek CSJ. Macromol Sci Phys 1973;B7(1):157–75.
[23] Blackwell J, Gardner KH. Polymer 1979;20:13.
[24] Koberstein JT, Gancarz IJ. Polym Sci Polym Phys 1986;24:2487.

[25] Lee HS, Hsu SL. Macromolecules 1989;22:1100.
[26] Brunette CM, Hsu SL, MacKnight WJ. Macromolecules 1982;15:71–7.
[27] Coleman MM, Lee KH, Skrovanek DJ, Painter PC. Macromolecules 1986;19:2149–57.
[28] Ning L, De-Ning W, Shenk-Kang Y. Macromolecules 1997;30: 4405–9.
[29] Sheth JP, Klinedinst DB, Wilkes GL, Yilgor I, Yilgor E. Polymer 2005; 46:7317–22.
[30] Sheth JP, Klinedinst DB, Pechar TW, Wilkes GL, Yilgor E, Yilgor I. Macromolecules 2005;38:10074–9.
[31] Tyagi D, Yilgor I, McGrath JE, Wilkes GL. Polymer 1984;25:1807–16.
[32] Klinedinst DB, Yilgor E, Yilgor I, Beyer FL, Wilkes GL. Polymer 2005; 46:10191–201.
[33] Coleman MM, Painter PC. Prog Polym Sci 1995;20:1–59.
[34] Coleman MM, Skrovanek DJ, Hu J, Painter PC. Macromolecules 1988; 21(1):59–66.
[35] Garrett JT, Xu R, Cho J, Runt J. Polymer 2003;44:2711–9.
[36] Sheth JP, Aneja A, Wilkes GL, Yilgor E, Atilla GE, Yilgor I, Beyer FL. Polymer 2004;45:6919–32.
[37] Wang CB, Cooper SL. Macromolecules 1983;16:775–86.
[38] Lee HS, Wang YK, Hsu SL. Macromolecules 1987;20:2089–95.
[39] Teo LS, Chen CY, Kuo JF. Macromolecules 1997;30:1793–9.